CHEMISTRY
A EUROPEAN JOURNAL

ChemPubSoc
Europe

DOI: 10.1002/chem.201202140

Studies on the Amination of Aryl Chlorides with a Monoligated Palladium Catalyst: Kinetic Evidence for a Cooperative Mechanism

Ciril Jimeno,*[a] Ute Christmann,[b] Eduardo C. Escudero-Adán,[b] Ramon Vilar,[c] and Miquel A. Pericàs*[b, d]

Abstract: Combined spectroscopic, crystallographic, and kinetic studies of the mechanism of aromatic amination with the efficient dinuclear Pd precatalyst [$Pd_2Cl(\mu\text{-}Cl)PtBu_2$(Bph-Me)] (Bph-Me = 2′-methyl-[1,1′-biphenyl]-2-yl) have revealed overlapping, yet cooperative, mechanistic scenarios, the relative weights of which are strongly influenced by the products formed as the reaction proceeds. The stability and evolution of the precatalyst in solution has been studied and several metalation pathways that point to a single monoligated intermediate have been identified. Our work sheds light on the nature of the catalytic species involved in the process and on the structure of the corresponding catalytic network.

Keywords: amination · C–H activation · cross-coupling · palladium · reaction mechanisms

Introduction

The development of monoligated palladium catalysts for cross-coupling reactions has led to an extraordinary variety of efficient synthetic methods of proven reliability.[1] Palladium-catalyzed amination of aryl halides is of particular interest because it provides direct access to valuable nitrogen-containing fine chemicals and pharmaceuticals.[2] Bulky, electron-rich biaryl phosphanes, developed by Buchwald and co-workers, are particularly useful for this transformation because fine-tuning of the structure can accelerate all of the elementary steps within the catalytic cycle.[3] Indeed, several types of sterically hindered trialkylphosphines can also be used for this purpose.[4–7] These monophosphine ligands have expanded and complemented the scope of C–N coupling reactions, in competition with classical Pd–bidentate phosphine complexes.[8–12]

In view of their practical interest, numerous detailed mechanistic and kinetic investigations that deal with C–N bond formation catalyzed by diphosphine–palladium complexes have appeared in the literature.[9–12] However, comprehensive studies on the catalytic cycle with monophosphine complexes are much rarer[13] and mostly focus on elucidation of the nature of the active catalyst.[14] On this point, there has been some consensus that monoligated phosphine–Pd complexes are the real catalytic species.[13–15] Isolation and characterization of palladium intermediates has also been used to track potential catalytic pathways for such monophosphine–palladium systems.[16,17] Very recently, the reactivity and stability of dimeric monophosphine–Pd^I complexes, such as [($PtBu_3$)PdBr]$_2$, in Suzuki cross-coupling has been studied experimentally and theoretically, which confirmed that monomeric Pd^0 species formed by a reductive pathway, and not bimetallic- or monomeric Pd^I species, operate in the most likely scenario.[18]

We have previously reported[19] that the dinuclear Pd complex **1** [$Pd_2Cl(\mu\text{-}Cl)PtBu_2$(Bph-Me)] (Bph-Me = 2′-methyl-[1,1′-biphenyl]-2-yl), which contains a single biarylphosphine ligand (Scheme 1), shows outstanding catalytic activity without an induction period in amination reactions

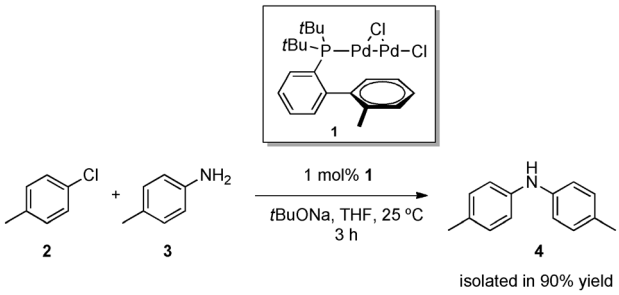

Scheme 1. Amination of **2** catalyzed by **1**.

[a] Dr. C. Jimeno
Department of Biological Chemistry and Molecular Modelling
Institute of Advanced Chemistry of Catalonia (IQAC-CSIC)
Jordi Girona 18-26, 08034 Barcelona (Spain)
E-mail: ciril.jimeno@iqac.csic.es

[b] Dr. U. Christmann, E. C. Escudero-Adán, Prof. M. A. Pericàs
Institute of Chemical Research of Catalonia (ICIQ)
Av. Països Catalans 16, 43007 Tarragona (Spain)
E-mail: mapericas@iciq.es

[c] Prof. R. Vilar
Department of Chemistry, Imperial College London
South Kensington, London SW7 2AZ (UK)

[d] Prof. M. A. Pericàs
Departament de Química Orgànica, Universitat de Barcelona
Martí i franquès 1-11, 08028 Barcelona (Spain)

Supporting information for this article is available on the WWW under http://dx.doi.org/10.1002/chem.201202140.

of aryl chlorides at room temperature. It was proposed that bimetallic **1** readily generates the monometallic species [Pd(P*t*Bu$_2$)(Bph-Me)] in situ, which acted as the true catalyst in the amination reaction.

Herein, we describe spectroscopic, crystallographic, and kinetic studies of the mechanism of the amination of *p*-chlorotoluene (**2**) with *p*-toluidine (**3**) catalyzed by **1** (1 mol%) at room temperature (Scheme 1). Although aryl chlorides are very unreactive electrophiles and anilines are poorly coordinating bases, the amination catalyzed by complex **1** is a clean reaction, not complicated by the formation of triarylamine byproducts; the reaction is essentially complete within 3 h under the reaction conditions studied.[19b]

Cross-coupling reactions are generally assumed to proceed through simple oxidative addition/reductive elimination mechanisms and the potential appearance of secondary cycles at high conversions due to the increasing concentration of species formed during the reactions are normally overlooked. In this paper, we propose a mechanistic model that accounts for the observed kinetic behavior over the whole reaction and shows that a secondary catalytic cycle has to be taken into account at high conversion. This behavior might also be operative in other cross-coupling reactions catalyzed by monophosphine palladium complexes.

Results and Discussion

Spectroscopic and structural studies on the stability and evolution of precatalyst 1 under the selected reaction conditions: The high catalytic activity displayed by **1** suggests that not only isolation, but also in situ detection and characterization, of the catalytically active species and resting state of the catalyst might be exceedingly challenging. Nonetheless, we studied the evolution of **1** in the presence of the isolated reactants (or combinations thereof) by $^{31}P\{^1H\}$ NMR spectroscopy and X-ray crystallography (see the Supporting Information) to rationalize the conversion of precatalyst **1** into the catalytically active species and to understand its stability under the actual reaction conditions.

We found that **1** was unreactive toward **2** at 25°C, despite that one of the two Pd atoms in **1** is formally zero valent and that the catalytic amination readily occurs at room temperature. Thus, both the dark-green color of the solution and the ^{31}P NMR spectrum ($\delta = 59.3$ ppm) of **1** remained unchanged upon addition of **2**. In contrast, the addition of NaO*t*Bu (4.6 equiv) to **1** resulted in an immediate color change to deep red. Also, two new singlet resonances appeared in the ^{31}P NMR spectrum, one at $\delta = 53.7$ ppm (major), which could correspond to the putative monoligated Pd^0 species or a **1**·O*t*Bu complex,[20] and one at $\delta =$ 23.1 ppm (minor), which corresponded to the free ligand P*t*Bu$_2$(Bph-Me).[19] It is worth mentioning that the observation of free phosphine under these conditions, together with the precipitation of palladium black, provides a clear hint on the formation of the active species and on its decomposition mode in the absence of additional reagents (Scheme 2).

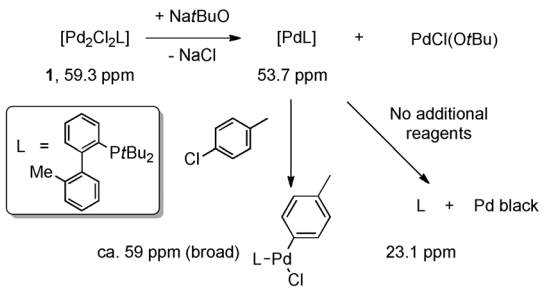

Scheme 2. ^{31}P NMR spectroscopic studies on the activation of **1**.

A similar change in the ^{31}P NMR spectral pattern was observed when NaO*t*Bu was added to a solution of **1** containing **2**, except that no resonance from free P*t*Bu$_2$(Bph-Me) could be seen. In this case, the signal attributed to the monoligated Pd^0 species ($\delta = 53.7$ ppm) was accompanied by a broad resonance at $\delta \approx 59$ ppm. According to close precedent,[21] this peak could correspond to the oxidative-addition product.[22] On the other hand, the addition of **3** or a combination of **3** and NaO*t*Bu to **1** led to complex ^{31}P NMR spectral patterns, indicative of non-selective transformations, and was accompanied by the formation of considerable amounts of free P*t*Bu$_2$(Bph-Me) ligand and palladium black. Thus, the very clean reaction promoted by **1** under the actual catalytic conditions clearly suggests that the activation of the precatalyst is initiated by interaction with NaO*t*Bu, which triggers formation of the catalytically active species, and that interaction with **3** only occurs after the oxidative-addition step (Scheme 2). These results are in agreement with Buchwald's calorimetric and ^{31}P NMR spectroscopic measurements on the activation of several Pd precatalysts by base, which showed that activation occurs readily at 80°C with weak bases like K_2CO_3, at RT with NaO*t*Amyl, and even at −20°C with metal hexamethyldisilazides (HMDS).[15]

Complementary information was obtained from X-ray analysis of crystalline materials that deposited in low yield from the samples described above. Thus, the reaction of **1** with **3** gave rise to the known[19] cyclometalated dimer **6** (Figure 1). A remarkable, previously unreported isomer of **6** was identified by single-crystal X-ray diffraction to be among the products of the reaction of **1** with **2** and NaO*t*Bu.

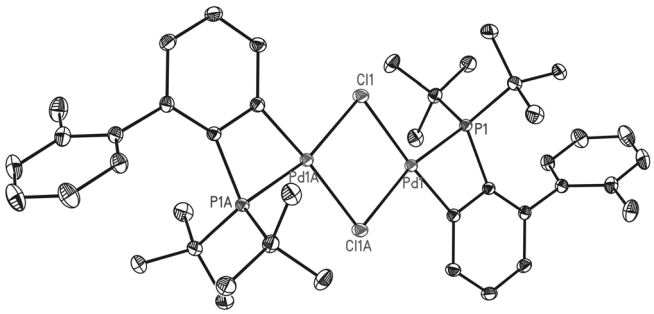

Figure 1. ORTEP drawing of complex **6** with thermal ellipsoids set at the 50% probability level. All hydrogen atoms have been omitted for clarity.

This complex (**7**), a result of cyclometalation at the aromatic CH_3 group of the Bph-Me ligand, displays an unusual seven-membered palladacycle moiety (Figure 2). Interestingly, another crystal from the same sample (see the Supporting Information for details) was comprised from **7** (ca. 70%) co-crystallized with its doubly OH-bridged analogue (ca. 30%), produced by hydrolysis of **7** with adventitious H_2O. Finally, we determined an X-ray structure of the cyclic phosphonium salt **9** with $[Pd_2Cl_6]^{2-}$ as the counterion (Figure 3), likely formed by cyclopalladation of the aromatic *ortho* C–H bond, followed by reductive elimination (Scheme 3).[23]

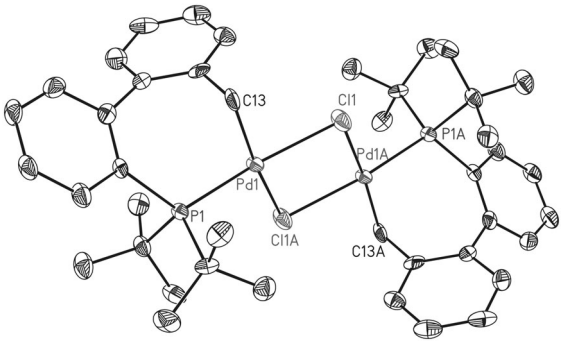

Figure 2. ORTEP drawing of complex **7** with thermal ellipsoids set at the 50% probability level. All hydrogen atoms have been omitted for clarity.

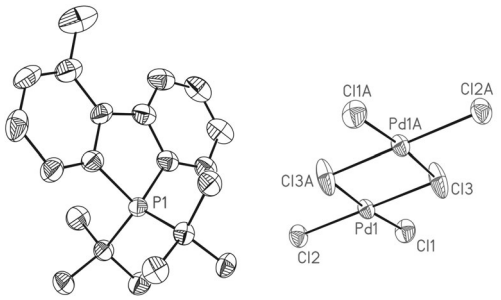

Figure 3. ORTEP drawing of phosphonium salt **9** with thermal ellipsoids set at the 50% probability level. All hydrogen atoms have been omitted for clarity.

It is interesting to realize that the diversity of the observed C–H activation reactions undergone by the phosphine ligand in complex **1** can be tracked back to closely related Pd^{II} intermediates that arise either from the decomposition of precatalyst **1** to **5** (X = Cl) plus palladium black,[19b] or from the oxidative-addition intermediate (**5**, X = Ar) in the cross-coupling catalytic cycle (Scheme 3). Although both putative intermediates **5** are likely precursors of **6**, **7**, and **9**, it is experimentally known that under the actual amination reaction conditions cross-coupling is much faster than any potential C–H activation decomposition pathways.[24]

Kinetic analysis: Kinetic studies were conducted by continuous monitoring of the reaction shown in Scheme 1 by in situ

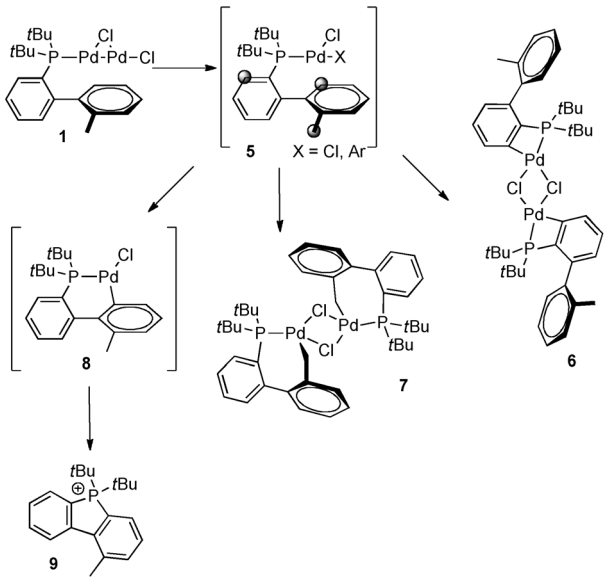

Scheme 3. Rationalization of the formation of palladacycles **6** and **7** and phosphonium salt **9** from **1**.

FTIR spectroscopy under synthetically relevant conditions up to full conversion. Initially, the amount of base and stirring speed were optimized to ensure homogeneity (see the Supporting Information for details).[25,26] Data collected were analyzed by following Blackmond's method,[27] which has proven to be particularly reliable for cross-coupling reactions and allows extraction of information throughout the entire reaction under realistic conditions, thus avoids the use of pseudo-zero-order conditions, high dilutions, or initial-rate measurements that might give rise to conclusions that are difficult to translate into practical systems.

In Figure 4a, plots of rate versus concentration of **2** are represented for three runs at different initial concentrations of **2** and **3**. In all cases, the reaction rates were high at the beginning but suffered a pronounced decrease after approximately 50% conversion was reached. The plots of the reactions with different initial concentrations but the same excess ($[e] = [\mathbf{3}]_0 - [\mathbf{2}]_0$) do not overlay at the beginning. Importantly, the reaction was faster at lower rather than higher concentrations of the reactants. This observation suggested either catalyst deactivation or product inhibition.[27] An additional experiment was carried out by adding a known amount of product **4** to the reaction mixture (10 mol%). The reaction rate in the presence of **4** was lower, indicative of product inhibition (see the Supporting Information for details). It is noteworthy that although product inhibition has been observed by Hartwig et al. in $[Pd(BINAP)_2]$ (BINAP = 2,2′-bis(diphenylphosphino)-1,1′-binaphthyl) catalyzed amination reactions,[9c] we are unaware of other reports of this effect in cross-coupling aminations.[28]

Figure 4b displays plots of the catalyst turnover frequency (TOF) versus concentration of **2** for two runs with different catalyst concentrations. These plots overlay, which indicates that the catalyst is stable throughout the process and that the reaction is first order with respect to **1**.[27]

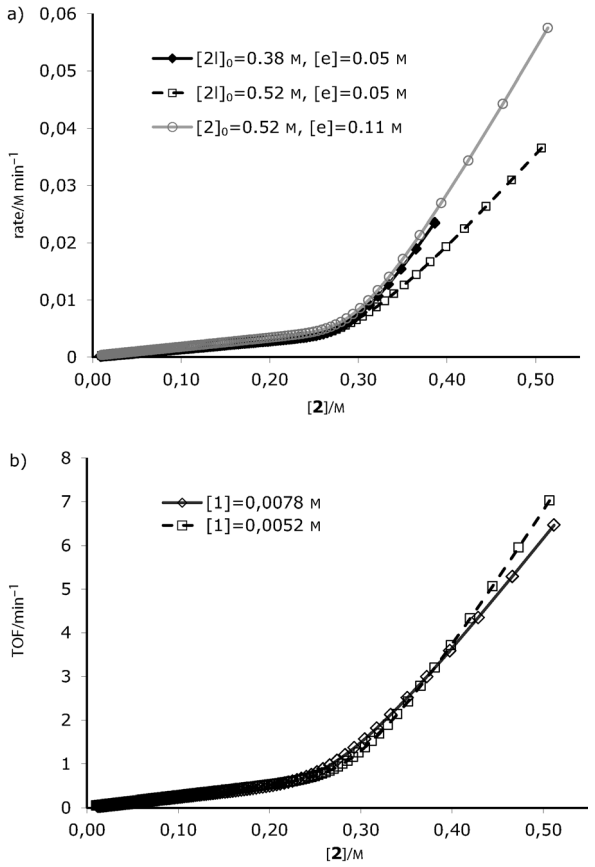

Figure 4. a) Plot of rate versus [**2**]. b) Plot of catalyst TOF versus [**2**]. Conversion increases from right to left.

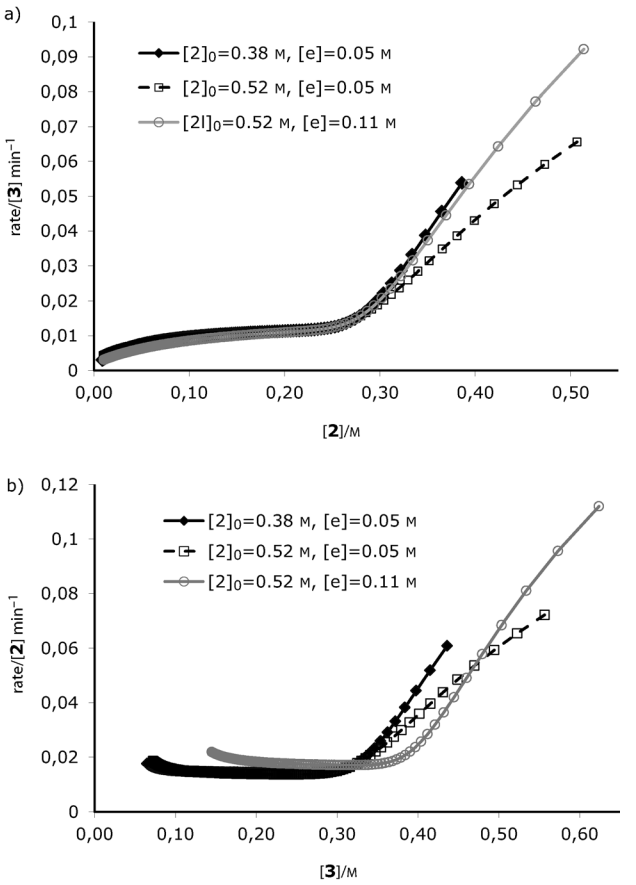

Figure 5. a) Plot of rate/[**3**] versus [**2**]. b) Plot of rate/[**2**] versus [**3**]. Conversion increases from right to left.

Further analysis of the data shown in Figure 4a led to important conclusions. By normalizing the reaction rate by the concentrations of **2** and **3**, the dependencies on both reactants could be analyzed (Figure 5). It became clear that two different "reaction regions" were operative. Figure 5a shows the plot of rate/[**3**] against [**2**]. It is apparent that the plots overlay in the left-hand region (high conversion), but not in the right-hand region (low conversion), which indicates complex behavior. The curve shape suggested saturation kinetics in **2** at high conversion, confirmed by reciprocal plots of these data (see the Supporting Information).

The plot of rate/[**2**] against [**3**] exhibited a similar behavior (Figure 5b). Again, the curves did not overlay in the low-conversion region. At higher conversion, the plots overlayed, but the almost-perfect flat shape indicated the reaction to be zero order with respect to **3**. The non-overlaying areas of the curves are explicable if the product-inhibition effect described above is taken into account. The difference is more pronounced at the beginning of the reactions when the differences in reaction rate are higher.

Mechanistic proposal: The kinetic investigations gave an indication of the steps involved in the mechanism:

1) the catalyst was stable throughout the reaction and the rate was first order with respect to catalyst concentration.
2) at initial rates and up to almost 50% conversion (right-hand side of the plots in Figures 4 and 5) product inhibition was detected and dependencies on reactant concentrations indicated saturation kinetics for both **2** and **3**.
3) beyond 50% conversion to the end of the reaction (left-hand side of the plots in Figures 4 and 5), saturation kinetics for **2** and zero-order dependency on **3** were found.

To shed light on this apparently complex behavior, exhaustive kinetic modeling was carried out.[29] Simple catalytic cycles did not provide reasonable fittings, even with product inhibition. Eventually, two interconnected catalytic cycles were required fit all of the experimental data (Figure 6). The use of models that involved these two cycles arose from consideration of the interaction of chloride anions (formed in the reaction) with the active catalytic species to generate a secondary anionic cycle that would operate simultaneously.[30] Obviously, the concentration of chloride anions increases as the reaction proceeds and, therefore, the relative weight of this secondary cycle must increase in parallel. Indeed, anionic Pd species have been proposed to

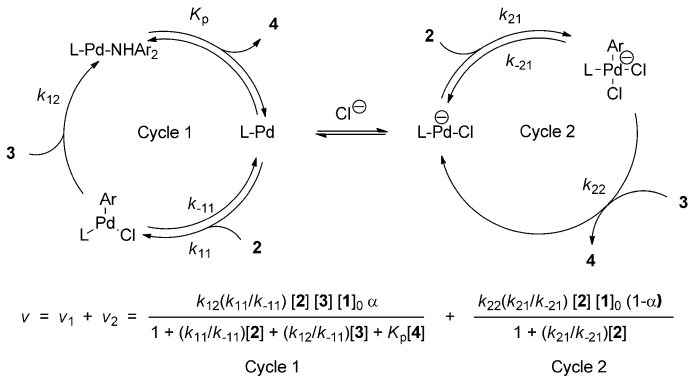

Figure 6. General kinetic model for two interdependent cycles shifting throughout time, and model equations used for the fitting. The value of α can vary between 0 and 1.

be catalytically active;[13,26,31] in particular, the effect of chloride anions cannot be disregarded.[28]

The first cycle includes oxidative addition of **2**, binding of **3**, and reductive elimination of **4**. The observed product inhibition is taken into account to yield the first rate equation (v_1)[27] that corresponds to the behavior observed predominantly at the beginning of the amination reaction. This means that neither a well-defined rate-limiting step, nor a catalyst resting state, is involved in the process.

A much simpler rate equation (v_2) corresponds to the second cycle (the predominant behavior at the end of the amination reaction), in which there is zero-order kinetics with respect to **3**.[27] The two cycles are linked by means of a factor that varies as the reaction progresses; different weights are given to v_1 and v_2 depending on the needs of the fitting (Figure 6). This is mathematically expressed by using the partition factor (α). The implications of such a parameter will be discussed later.

Simultaneous optimization of conversion-dependent α and the kinetic equation parameters produced an excellent fit to the experimental data (Figure 7).[29] It should be emphasized that as long as the catalyst does not decompose (Figure 4b) its overall concentration is constant throughout the process (as in the model used), regardless of how many different catalytically active species are involved.

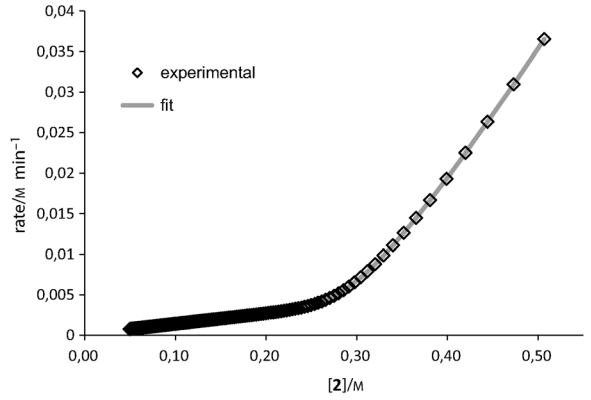

Figure 7. Model fitting to the experimental data and calculated kinetic parameters by the least-squares method; $k_{11}/k_{-11} = 1.66(\pm0.02)\,M^{-1}$; $k_{12} = 30.8(\pm0.3)\,M^{-1}min^{-1}$; $K_P = 1.86(\pm0.02)\,M^{-1}$; $k_{21}/k_{-21} = 19.9(\pm0.2)\,M^{-1}$; $k_{22} = 0.33(\pm0.01)\,M^{-1}min^{-1}$.

It is also worth comparing the values of the rate constants involved in the model. The oxidative-addition step for an anionic pathway should be faster than for a neutral one, as found in the model; k_{21}/k_{-21} is one order of magnitude bigger than k_{11}/k_{-11} (19.9 versus $1.66\,M^{-1}$). At the same time, reductive elimination should be faster for a neutral cycle; indeed k_{12} is two orders of magnitude bigger than k_{22}, although, in this case, some caution must be assumed because the values obtained from the model constants combine amine binding and reductive elimination.

At this point, the α-factor evolution was analyzed to verify the quality of the model because a random or illogical evolution would indicate a pointless mechanistic proposal, regardless of the quality of the fitting. Figure 8 shows a plot of α versus the concentration of **2**. The constant smoothly decays from 1 to 0.30 at approximately 50% conversion

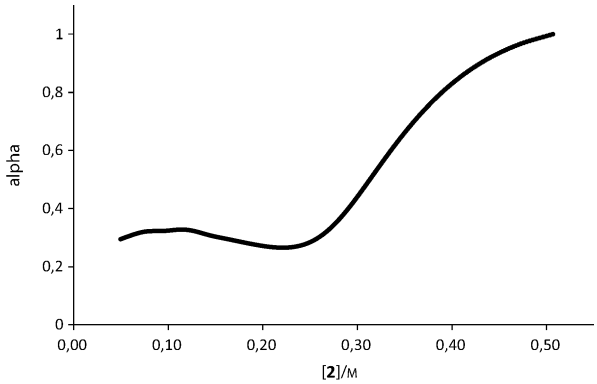

Figure 8. Evolution of α with reaction progress (from right to left).

(only cycle 1 in operation; Figure 6), then stays at approximately this value until the end of the reaction. From a chemical perspective, the evolution of α indicates that the second catalytic cycle becomes more important over time, with the contribution of its active catalyst to the overall process increasing up to 70% $\{[\mathbf{1}]_0(1-\alpha)\}$. As already discussed, the observed trend is in agreement with the formation of a new catalytic species from the original catalyst as the reaction proceeds toward completion. The stabilization of the value of α at high conversion is in agreement with saturation of the solution with chloride ions in the late stages of the reaction.

An alternative illustration of the mechanism that involves two catalytic cycles comes from components analysis of the reaction rate. By plotting the rates of both cycles illustrated in Figure 6 (v_1 and v_2) versus the concentration of **2**, their contributions to the overall reaction rate can be visualized (Figure 9). It can be seen from Figure 9 that cycle 1 predominates at the beginning of the reaction. Approaching approximately 50% conversion, cycle 2 gains more weight, and from then onwards contributes equally to the overall rate and even surpasses the contribution of cycle 1 at the end of the reaction. After 50% conversion, $\alpha \approx 0.30$, which means that the amount of active palladium species involved in

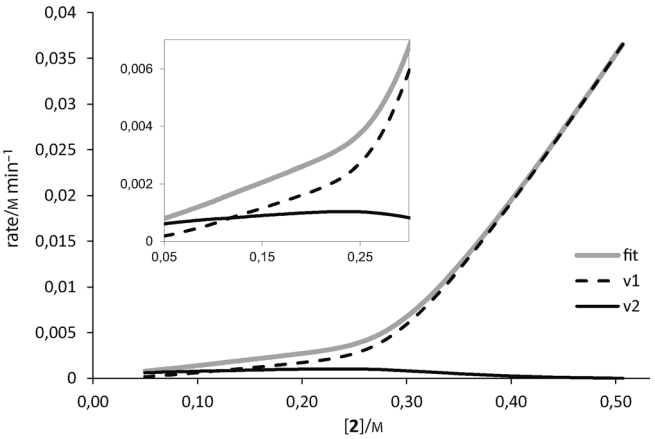

Figure 9. Components analysis of the reaction rate. Inset: expansion of the profiles at higher conversion (conversion increases from right to left).

cycle 2 exceeds that operating in cycle 1. Nonetheless, both cycles contribute similarly to the overall reaction rate because cycle 2 is intrinsically slower than cycle 1, which can seen from the rate constants for the irreversible reaction steps ($k_{12}=30.8$ versus $k_{22}=0.33\,\text{M}^{-1}\,\text{min}^{-1}$).

Although anionic cycles based on chloride binding are usually faster than neutral mechanisms,[32] it seems that in this particular case only the oxidative addition is accelerated. This would lead to an overall slower secondary cycle that would eventually predominate due to the increasing concentration of chloride ions. To confirm this hypothesis, sodium chloride (10 mol% with respect to **2**) was added at the beginning of the reaction and a marked decrease in the rate of product formation was observed. Moreover, almost total inhibition was observed when tetrabutylammonium chloride (a fully soluble source of chloride anions) was used as an additive (see the Supporting Information for details). To discount any effect due to the tetrabutylammonium cation,[33] an additional experiment was performed in the presence of lithium chloride (20 mol%), which is more soluble in THF. Inhibition was again observed; conversion after 1 h decreased from 54% (control experiment) to 34%.[34–36] Thus, these results strongly indicate that the interaction of chloride anions with the catalyst leads to an alternative, slower mechanism, which is in full agreement with the kinetic studies reported above.

Conclusion

The amination of *p*-chlorotoluene (**2**) with *p*-toluidine (**3**) in the presence of the dinuclear palladium complex **1** involves a complex mechanistic scenario. According to the kinetic analysis, the reaction is subject to product inhibition and two distinct catalytic cycles are involved in the overall process. The two cycles contribute differently to the formation of the final product. Additionally, their contributions change continuously as the reaction progresses. The appearance of chloride anions in the medium as one of the reaction products leads to a new anionic catalytic species that makes the secondary cycle gain importance with time. For this reason, both cycles appear to be linked throughout the reaction progress in a cooperative way: the rate decrease of the regular neutral cycle as conversion increases is compensated by the secondary anionic cycle.

It is believed that both cycles 1 and 2 involve mononuclear Pd species; these species could not be identified because of their exceptionally high reactivity. Deduced from the ^{31}P NMR spectroscopic and X-ray diffraction studies reported here, one of the two Pd atoms of **1** is easily lost upon addition of NaO*t*Bu—the base used in stoichiometric quantities in the catalytic process and a key element for the outstanding reactivity of **1** in amination reactions.

The stability of the catalyst has been also addressed. It has been found that in the absence of substrates to process, the active catalytic species readily experiences cyclopalladation with geometrically available C–H bonds in the phosphine ligand. This could be a common mechanism of decomposition for Pd–monophosphine ligand complexes.

Although detailed structural information on catalytically active species derived from **1** could not be obtained, our work provides valuable information and guidelines for further studies (e.g. by computational means). Our results also bear implications for further improvements to the valuable aromatic amination reaction by suppression of product inhibition in the primary catalytic cycle and the slower, yet active, secondary cycle. It is likely that secondary anionic catalytic cycles also operate in other amination reactions catalyzed by palladium complexes. These slower, yet important, catalytic reaction pathways were apparently unnoticed in previous kinetic studies that focused only on initial rates of reaction.

Experimental Section

Typical kinetic experiment: Reagents and precatalyst **1** were stored in a glovebox, and anhydrous solvents were used. Reactions were carried out in a jacketed, three-necked, heart-shaped glass reactor thermostatized at 25°C. Measurements were taken with an in situ ReactIR apparatus equipped with a diamond probe immersed in the reaction mixture. A representative signal corresponding to product formation ($\tilde{\nu}=1611\ \text{cm}^{-1}$) was tracked. The reaction vessel was heated at 110°C for 1 h under a nitrogen flow, then cooled to 40°C and the background IR spectrum was collected. Sodium *tert*-butoxide (534 mg, 5.56 mmol) and catalyst **1** (16.6 mg, 0.0278 mmol) were introduced. The vessel was simultaneously purged with nitrogen and cooled to 25°C. A solution of **2** (329 μL, 2.78 mmol) and **3** (328 mg, 3.06 mmol) in anhydrous THF (5 mL) was added by syringe under vigorous stirring (1000 rpm). Recording of the IR spectra was started immediately after the addition.

Acknowledgements

This work was funded by MINECO (grants CTQ2008–00947/BQU and CTQ2012–38594-C02–01), DEC (Grant 2009SGR623), and the ICIQ Foundation. C.J. thanks MICINN for a Ramón y Cajal contract. We thank Profs. V. Grushin and R. Martin (ICIQ) for helpful discussions, technical assistance, and the generous gift of reagents.

[1] U. Christmann, R. Vilar, *Angew. Chem.* **2005**, *117*, 370; *Angew. Chem. Int. Ed.* **2005**, *44*, 366.
[2] a) D. S. Surry, S. L. Buchwald, *Chem. Sci.* **2011**, *2*, 27; b) D. S. Surry, S. L. Buchwald, *Angew. Chem.* **2008**, *120*, 6438; *Angew. Chem. Int. Ed.* **2008**, *47*, 6338; c) S. L. Buchwald, C. Mauger, G. Mignani, U. Scholz, *Adv. Synth. Catal.* **2006**, *348*, 23.
[3] a) D. W. Old, J. P. Wolfe, S. L. Buchwald, *J. Am. Chem. Soc.* **1998**, *120*, 9722; b) X. Huang, K. W. Anderson, D. Zim, L. Jiang, A. Klapars, S. L. Buchwald, *J. Am. Chem. Soc.* **2003**, *125*, 6653; c) K. W. Anderson, M. Mendez-Perez, J. Priego, S. L. Buchwald, *J. Org. Chem.* **2003**, *68*, 9563; d) D. Zim, S. L. Buchwald, *Org. Lett.* **2003**, *5*, 2413; e) M. D. Charles, P. Schultz, S. L. Buchwald, *Org. Lett.* **2005**, *7*, 3965; f) K. W. Anderson, R. E. Tundel, T. Ikawa, R. A. Altman, S. L. Buchwald, *Angew. Chem.* **2006**, *118*, 6673; *Angew. Chem. Int. Ed.* **2006**, *45*, 6523; g) D. Maiti, B. P. Fors, J. L. Henderson, Y. Nakamura, S. L. Buchwald, *Chem. Sci.* **2011**, *2*, 57.
[4] a) J. F. Hartwig, M. Kawatsura, S. I. Hauck, K. H. Shaughnessy, L. M. Alcazar-Roman, *J. Org. Chem.* **1999**, *64*, 5575; b) J. P. Stambuli, R. Kuwano, J. F. Hartwig, *Angew. Chem.* **2002**, *114*, 4940; *Angew. Chem. Int. Ed.* **2002**, *41*, 4746.
[5] M. Prashad, X. Y. Mak, Y. Liu, O. Repic, *J. Org. Chem.* **2003**, *68*, 1163.
[6] L. L. Hill, J. L. Crowell, S. L. Tutwiler, N. L. Massie, C. C. Hines, S. T. Griffin, R. D. Rogers, K. H. Shaughnessy, *J. Org. Chem.* **2010**, *75*, 6477.
[7] a) S. Shekhar, J. F. Hartwig, *Organometallics* **2007**, *26*, 340; b) F. Barrios-Landeros, B. P. Carrow, J. F. Hartwig, *J. Am. Chem. Soc.* **2009**, *131*, 8141.
[8] a) Q. Shen, J. F. Hatwig, *J. Am. Chem. Soc.* **2006**, *128*, 10028; b) Q. Shen, T. Ogata, J. F. Hartwig, *J. Am. Chem. Soc.* **2008**, *130*, 6586; c) T. Ogata, J. F. Hartwig, *J. Am. Chem. Soc.* **2008**, *130*, 13848; d) Q. Shen, J. F. Hartwig, *Org. Lett.* **2008**, *10*, 4109; e) J. F. Hartwig, *Acc. Chem. Res.* **2008**, *41*, 1534; f) G. D. Vo, J. F. Hartwig, *J. Am. Chem. Soc.* **2009**, *131*, 11049.
[9] a) S. Shekhar, P. Ryberg, J. F. Hartwig, J. S. Mathew, D. G. Blackmond, E. R. Strieter, S. L. Buchwald, *J. Am. Chem. Soc.* **2006**, *128*, 3584; b) U. K. Singh, E. R. Strieter, D. G. Blackmond, S. L. Buchwald, *J. Am. Chem. Soc.* **2002**, *124*, 14104; c) L. M. Alcazar-Roman, J. F. Hartwig, A. L. Rheingold, L. M. Liable-Sands, I. A. Guzei, *J. Am. Chem. Soc.* **2000**, *122*, 4618.
[10] L. M. Klingensmith, E. R. Strieter, T. E. Barder, S. L. Buchwald, *Organometallics* **2006**, *25*, 82.
[11] B. C. Hamann, J. F. Hartwig, *J. Am. Chem. Soc.* **1998**, *120*, 7369.
[12] G. Mann, J. F. Hartwig, *J. Am. Chem. Soc.* **1996**, *118*, 13109.
[13] L. M. Alcazar-Roman, J. F. Hartwig, *J. Am. Chem. Soc.* **2001**, *123*, 12905.
[14] E. R. Strieter, D. G. Blackmond, S. L. Buchwald, *J. Am. Chem. Soc.* **2003**, *125*, 13978.
[15] M. R. Biscoe, B. P. Fors, S. L. Buchwald, *J. Am. Chem. Soc.* **2008**, *130*, 6686.
[16] a) M. R. Biscoe, T. E. Barder, S. L. Buchwald, *Angew. Chem.* **2007**, *119*, 7370; *Angew. Chem. Int. Ed.* **2007**, *46*, 7232; b) T. E. Barder, M. R. Biscoe, S. L. Buchwald, *Organometallics* **2007**, *26*, 2183.
[17] a) R. A. Widenhoefer, H. A. Zhong, S. L. Buchwald, *Organometallics* **1996**, *15*, 2745; b) R. A. Widenhoefer, S. L. Buchwald, *Organometallics* **1996**, *15*, 2755; c) R. A. Widenhoefer, S. L. Buchwald, *Organometallics* **1996**, *15*, 3534.
[18] F. Proutiere, M. Aufiero, F. Schoenebeck, *J. Am. Chem. Soc.* **2012**, *134*, 606.
[19] a) U. Christmann, R. Vilar, A. J. P. White, D. J. Williams, *Chem. Commun.* **2004**, 1294; b) U. Christmann, D. A. Pantazis, J. Benet-Buchholz, J. E. McGrady, F. Maseras, R. Vilar, *J. Am. Chem. Soc.* **2006**, *128*, 6376.
[20] Studies aimed at elucidation of the nature of this species are currently underway in our laboratories.
[21] T. J. Maimone, P. J. Milner, T. Kinzel, Y. Zhang, M. T. Takase, S. L. Buchwald, *J. Am. Chem. Soc.* **2011**, *133*, 18106.
[22] Attempts to prepare the oxidative-addition complex **5** (X = Ar) by reaction of the corresponding phosphine with [Pd(cod)Me_2] (cod = 1,5-cyclooctadiene) and **2** yielded complex mixtures according to the $^{31}P\{^1H\}$ NMR spectra.
[23] A palladacyclic phosphine was successfully used as precatalyst for the amination of aryl chlorides; see ref. [3d].
[24] Attempts to identify palladacycle intermediates in the reaction mixture by ^{31}P NMR spectroscopic analysis were unsuccessful. For example, the chemical shift of **6** in [D_8]THF is −13.1 ppm; see ref. [19b].
[25] For a recent experimental and theoretical study on the amination with Pd/N-heterocyclic carbene complexes, with special emphasis on the effect of base and amine, see: K. H. Hoi, S. Çalimsiz, R. D. J. Froese, A. C. Hopkinson, M. G. Organ, *Chem. Eur. J.* **2011**, *17*, 3086.
[26] For a recent paper on solvent effects on the neutral/anionic nature of a Pd cross-coupling catalyst, see: F. Proutiere, F. Schoenebeck, *Angew. Chem.* **2011**, *123*, 8342; *Angew. Chem. Int. Ed.* **2011**, *50*, 8192.
[27] a) D. G. Blackmond, *Angew. Chem.* **2005**, *117*, 4374; *Angew. Chem. Int. Ed.* **2005**, *44*, 4302; b) J. S. Mathew, M. Klussmann, H. Iwamura, F. Valera, A. Futran, E. A. C. Emanuelson, D. G. Blackmond, *J. Org. Chem.* **2006**, *71*, 4711.
[28] For kinetic analysis of catalytic reactions that involve product inhibition, see: a) T. Rosner, P. J. Sears, W. A. Nugent, D. G. Blackmond, *Org. Lett.* **2000**, *2*, 2511; b) C. Jimeno, A. Vidal-Ferran, M. A. Pericàs, *Org. Lett.* **2006**, *8*, 3895.
[29] Optimization was carried out with the Solver programme, from Excel, by the least-squares method.
[30] A mechanism with concurrent anionic and neutral catalytic cycles was proposed due to the interaction of certain alkoxide bases with the catalyst, see refs. [7] and [13].
[31] It has been shown that even ligand-free anionic palladium species are intermediates in Heck reactions: B. P. Carrow, J. F. Hartwig, *J. Am. Chem. Soc.* **2010**, *132*, 79.
[32] For mechanistic studies on the effect of chloride anions in palladium-catalyzed cross-coupling, Heck, and allylic substitution reactions, see: a) G. C. Lloyd-Jones, S. C. Stephen, *Chem. Commun.* **1998**, 2321; b) G. C. Lloyd-Jones, S. C. Stephen, *Chem. Eur. J.* **1998**, *4*, 2539; c) C. Amatore, A. Jutand, *Acc. Chem. Res.* **2000**, *33*, 314; d) C. Amatore, A. Jutand, *J. Organomet. Chem.* **1999**, *576*, 254; e) S. Kozuch, C. Amatore, A. Jutand, S. Shaik, *Organometallics* **2005**, *24*, 2319; f) A. Jutand, *Appl. Organomet. Chem.* **2004**, *18*, 574; g) P. Fristrup, T. Jensen, J. Hoppe, P.-O. Norrby, *Chem. Eur. J.* **2006**, *12*, 5352.
[33] D. S. Huang, J. F. Hartwig, *Angew. Chem.* **2010**, *122*, 5893; *Angew. Chem. Int. Ed.* **2010**, *49*, 5757.
[34] Seeking the opposite effect, an experiment was performed in the presence of $ZnCl_2$ (50 mol%), a potential chloride scavenger (see refs. [33] and [35]). However, a rate decrease was observed in this experiment (9% conversion after 1 h), which can be attributed to the operation of inhibitory pathways related to the Lewis acidity of zinc chloride in competition with its chloride-scavenging properties (see ref. [36]).
[35] Catalytic $ZnCl_2$ accelerates Sonogashira cross-coupling reactions. See: A. D. Finke, E. C. Elleby, M. J. Boyd, H. Weissman, J. S. Moore, *J. Org. Chem.* **2009**, *74*, 8897.
[36] The addition of $ZnCl_2$ suppresses Pd-catalyzed cross-coupling of Grignard reagents with vinyl bromide, whereas $ZnBr_2$ and ZnI_2 accelerate the reaction, see: G. Cross, B. K. Vriesema, G. Boven, R. M. Kellogg, *J. Organomet. Chem.* **1989**, *370*, 357–381.

Received: June 17, 2012
Revised: September 14, 2012
Published online: October 29, 2012

